Defect motifs for spherical topologies

David J. Wales and Hayley McKay
University Chemical Laboratories, Lensfield Road, Cambridge CB2 1EW, United Kingdom

Eric L. Altschuler
Departments of Physical Medicine and Rehabilitation and Microbiology & Molecular Medicine, University of Medicine & Dentistry of New Jersey, University Hospital, 150 Bergen Street, B-403, Newark, New Jersey 07103, USA

(Received 19 February 2009; published 22 June 2009)

Putative global minima for the Thomson problem of N charges on a sphere are located for selected sizes in the range $N \leq 4352$. For small sizes most global minima simply exhibit 12 disclinations. However, around $N=400$ extended dislocations are common, where a heptagon lies between two pentagons in the Voronoi representation. At larger sizes around $N=1000$ twinned grain boundaries are favorable and then between about $N=1000$ and 2000 "rosette" defects appear, containing a central pentagon surrounded by five heptagons alternating with five additional pentagons in the Voronoi representation. Structures with 12 rosettes and I point group symmetry are particularly low in energy for $N=1632$ and 1902. Above $N=2000$ the lowest minima located generally contain irregular grain boundaries, sometimes with a few rosette defects. Face dual carbon clusters corresponding to I_h local minima at $N=432$ and 582 are characterized as local minima for C_{860} and C_{1160}.

DOI: 10.1103/PhysRevB.79.224115 PACS number(s): 61.72.Mm, 02.60.Pn, 41.20.Cv, 61.72.Bb

I. INTRODUCTION

Many properties of atomic and mesoscale systems are determined by the presence of defects, especially the response to external forces, such as a mechanical load or an electric field.[1,2] For a spherical topology the presence of defects is unavoidable from geometrical considerations alone. If the number of neighbors for a particle in such a surface is written as C, then the topological or disclination charge is defined as $Q=6-C$. Euler's theorem states that the total disclination charge must be 12 for a triangulated structure defined by a set of particles constrained to a spherical surface. However, geometry alone does not tell us what the energetically favorable defect structures might be, and characterizing these arrangements is likely to play a key role in understanding and predicting the mechanical, optical, and electrical properties of such materials. Practical applications include the packing of spherical viruses,[3,4] fullerene structures,[5,6] multielectron bubbles in superfluid helium,[7,8] cell surface layers in prokaryotic organisms,[9,10] "colloidosomes,"[11–13] coding theory,[14,15] colloidal silica microspheres,[16] superconducting films,[17,18] micropatterning of spherical particles,[19] and lipid rafts deposited on vesicles.[20]

The simplest way for a triangulated lattice to achieve the required disclination charge is for 12 particles to form five-coordinate disclinations. However, packings with lower energy can be realized for larger systems via additional defects, which help to lower the strain energy. For example, dislocations may be formed from adjacent five-coordinate and seven-coordinate particles.[6,21,22] The importance of defects in explaining and predicting observable properties is highlighted in previous studies of disclinations,[23,24] dislocations,[6,18,22,25] and grain-boundary scars.[11,24,26] For example, dislocations are known to be important in the mechanical relaxation of carbon nanotubes, where a bond rotation in a hexagonal lattice wrapped around a cylindrical surface produces pentagon-heptagon pairs.[27] Dislocations may also contribute to the incorporation of new material into the surface layers of bacteria,[28] while disclinations may be involved in cell division.[29]

II. MODEL

Unfortunately, many systems of contemporary interest that exhibit spherical topologies are mesoscopic and cannot be modeled with a fully atomistic representation. However, useful insights have been obtained from analysis of the Thomson problem,[30] which consists of N unit charges constrained to a sphere with potential energy (atomic units)

$$V = \sum_{i<j} \frac{1}{|\mathbf{r}_i - \mathbf{r}_j|},$$

where the radius is $|\mathbf{r}_\alpha|=1$ for all particles α. This model was introduced by J. J. Thomson in 1904 to analyze atomic structure and has since been used as a testing ground for global optimization algorithms.[25,31–38] In a recent contribution[39] we employed the basin-hopping algorithm[40–44] to identify many improved candidates for global minima of the Thomson problem for $N \leq 400$. These structures included a variety of interesting defects. In the present contribution we describe trends in the observed defect structure up to $N=4352$.

III. RESULTS

The global potential energy minimum defines the equilibrium state of a classical system at sufficiently low temperatures and its influence often extends as far as a melting transition.[44] Characterizing this structure is therefore an important first step in many investigations throughout molecular science. The problem of finding the global minimum rapidly becomes more difficult as the system size increases, since the number of local minima increases exponentially

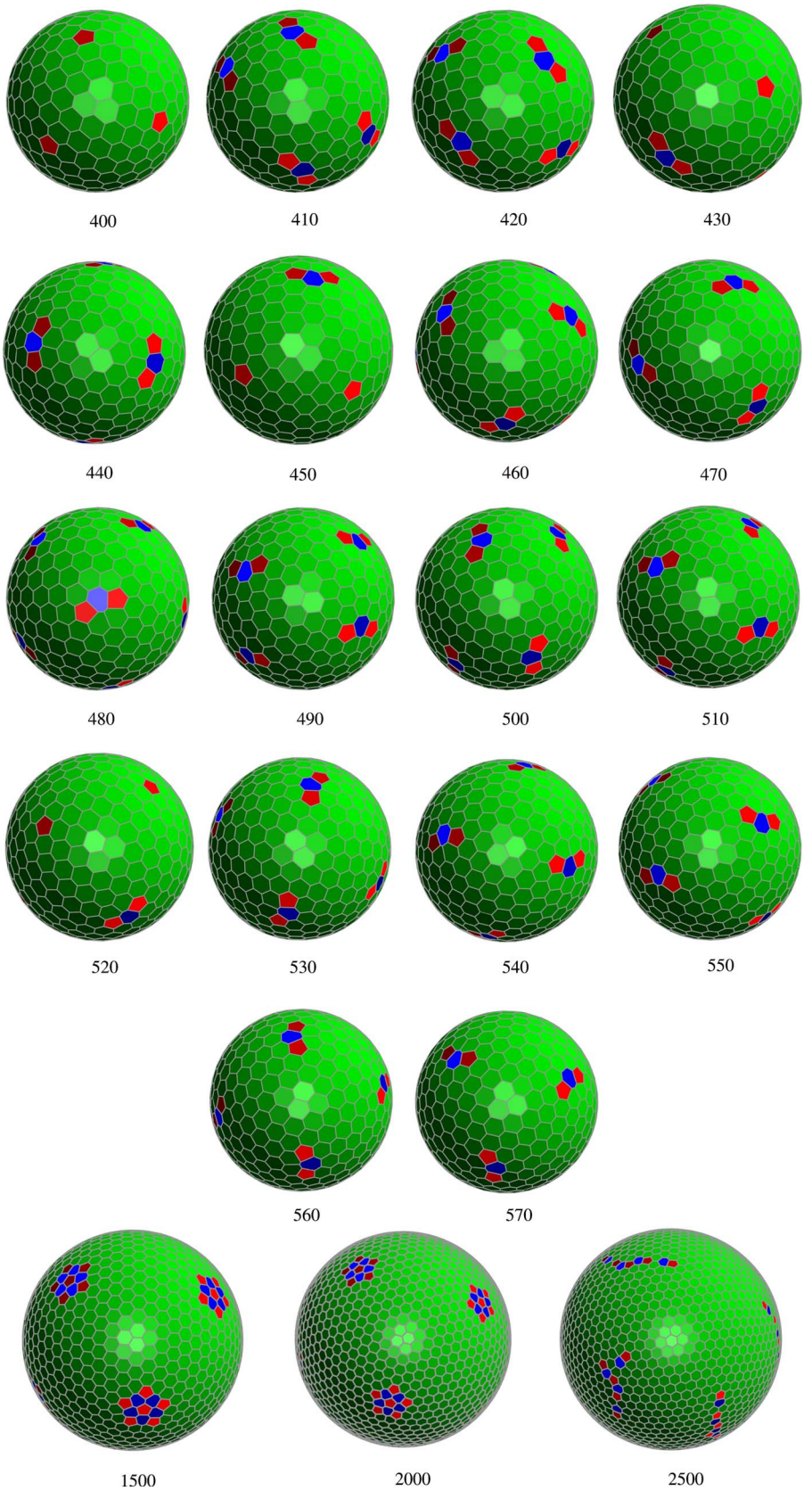

FIG. 1. (Color online) Voronoi representations of the lowest minima located for $N=400,410,\ldots,570$ and $N=1500$, 2000, and 2500. The pentagons, hexagons, and heptagons are colored red (medium gray), green (light gray), and blue (dark gray), respectively.

TABLE I. Lowest minima located for the Thomson problem at $N=400,410,\ldots,570$ and $N=1500$, 2000, and 2500. The number of polygons refers to faces with 5, 6, and 7 sides in the corresponding Voronoi construction.

N	Energy (a.u.)	$\frac{(2E-N^2)}{N^{3/2}}$	Point Group	Polygons		
				5	6	7
400	75582.4485122	−1.104388	T	12	388	0
410	79465.7432085	−1.104392	C_2	20	382	8
420	83446.9975989	−1.104394	C_2	24	384	12
430	87526.1187028	−1.104422	C_2	16	410	4
440	91703.3295563	−1.104428	D_2	24	404	12
450	95978.4413762	−1.104461	C_2	22	418	10
460	100351.7631087	−1.104458	T	24	424	12
470	104822.8863243	−1.104508	S_6	24	434	12
480	109392.3186786	−1.104513	C_1	24	444	12
490	114059.8425561	−1.104521	C_2	24	454	12
500	118825.4625421	−1.104535	C_2	24	464	12
510	123689.3168005	−1.104532	C_2	24	474	12
520	128651.1439930	−1.104563	C_2	22	488	10
530	133711.2618723	−1.104574	C_2	24	494	12
540	138869.5942030	−1.104582	C_2	24	504	12
550	144126.0927100	−1.104598	C_2	24	514	12
560	149480.8992800	−1.104602	D_2	24	524	12
570	154933.7024553	−1.104642	T_h	24	534	12
1500	1092900.8642237	−1.105062	C_1	66	1380	54
2000	1950575.6389387	−1.105162	C_1	58	1896	46
2500	3055924.2131105	−1.105213	C_1	61	2390	49

with the number of particles.[34,45,46] The rate of increase with size for the Thomson problem is not as large as for clusters bound by shorter-range potentials because the long-ranged Coulomb potential supports fewer local minima on the potential energy surface for any given size.[47–49] Nevertheless, the larger sizes considered in the present work pose a significant challenge. We first considered clusters with $N=1500$, 2000, and 2500. In each case we performed five separate basin-hopping runs starting from different randomly constructed arrangements for N particles on a sphere, using the GMIN program.[50] 50 000 basin-hopping steps were first performed at a fixed temperature of $T=0.045$, followed by an additional 50 000 steps at $T=0.06$. The energy range spanned by the lowest minima located in the five runs was 0.4 for $N=1500$, 1.0 for $N=2000$, and 0.6 for $N=2500$. The lowest minima improve upon previous results[51] by 4.6, 9.2, and 18.4 a.u., respectively. Our results therefore represent significantly better structures, but it is still possible that future studies will find slightly lower minima.

The lowest minima located at each size are illustrated in Fig. 1 using a Voronoi construction, based on polygons that partition the surface into regions where each point is closest to a given ion. In each case all the low-lying minima feature a number of "rosette" defects, where a central pentagon is surrounded by five heptagons alternating with five additional pentagons. The topological charge is equal to 12 for each structure (Table I), including the contributions from extended defects[25,26,39] consisting of pentagon/heptagon sequences that might be described as embryonic grain boundaries.[24,52]

Structures with 12 rosette defects and ideal I or I_h point group symmetry can be constructed using the standard triangulation number approach[3] by deleting a ring of sites around the 12 vertices of a regular icosahedron. The original construction produces lattices with point group I or I_h described by two integers, h and k, which correspond to displacements on a triangular lattice.[3] The number of vertices is then $10\Delta+2$ where $\Delta=h^2+hk+k^2$ is the triangulation number. Here we denote the geometry obtained by deleting a ring of sites by $(h,k)^-$ and the total number of vertices in this construction is $10\Delta-58$. Full I_h symmetry results if $h=0$, $k=0$, or $h=k$. Such structures have been considered before by Pérez-Garrido and Moore,[22] who constructed systems with icosahedral symmetry by removing sets of charges around 12 disclinations. They are also mentioned in a treatment that employs continuum elastic theory,[52] where families of "pentagonal buttons" are described with reference to unpublished work by A. Toomre.

In the present contribution we have considered all the systems based on 12 rosettes with I or I_h symmetry for systems with $N\leq 4352$, corresponding to $(0,21)^-$. There are 148

TABLE II. Lowest minima located for the Thomson problem at sizes corresponding to stable I or I_h minima from the $(0,k)^-$ series containing 12 rosette defects. The energy of the icosahedral minimum (E_I) and the lowest minimum (E_0) located from basin hopping are reported in each case in atomic units, together with the total number of basin-hopping steps.

N	E_I (12 rosettes)	E_0	E_I-E_0	$\frac{(2E_0-N^2)}{N^{3/2}}$	Point Group	Polygons 5	6	7
432	88360.9238182	88353.70968196	7.21414	−1.104425	D_3	24	395	12
582	161613.2267094	161607.1761347	6.05057	−1.104632	D_3	24	546	12
752	271365.3818886	271360.9889196	4.39297	−1.104754	C_2	24	716	12
942	427713.0332165	427710.4477820	2.58543	−1.104844	C_3	36	882	24
1152	641951.6761546	641950.0018189	1.67434	−1.104957	C_2	36	1092	24
1382	926576.7160510	926576.1175607	0.59849	−1.105020	C_1	57	1280	45
1632	1295282.2378931	1295282.2378931	0	−1.105112	I	72	1500	60
1902	1762965.4579074	1762965.4579073	0	−1.105162	I	72	1770	60
2192	2345723.5209933	2345722.2993502	1.22164	−1.105163	C_1	49	2106	37
2502	3060847.3069053	3060843.5371385	3.76977	−1.105209	C_1	75	2366	61
2832	3926833.9521952	3926826.0886472	7.86355	−1.105253	C_1	66	2712	54
3182	4963378.7006027	4963365.9063241	12.8738	−1.105286	C_1	68	3060	54
3552	6191369.8423152	6191357.2579633	12.4722	−1.105317	C_1	71	3422	59
3942	7632923.4474897	7632895.0289372	28.4186	−1.105350	C_1	73	3808	61
4352	9311298.8725923	9311276.2839985	22.5886	−1.105369	C_1	82	4202	68

such structures in this size range (excluding enantiomers) and local minimization with icosahedral symmetry enforced by a projection operator enabled us to obtain I or I_h symmetry stationary points for each possibility. However, for smaller sizes some of these structures correspond to saddle points rather than minima, as indicated by collapse to lower energy on tight optimization with no symmetry constraints. We finally characterized 26 minima with I_h symmetry and 113 with I symmetry.

To determine whether a 12-rosette motif is ever a likely candidate for the global minimum we conducted basin-hopping runs at fixed temperatures of $T=0.045$ and 0.06 for the sizes corresponding to $(h,0)^-$. At four of these sizes minima with I symmetry lie lower than I_h structures, namely, $N=1632$, 1902, 3552, and 4352, for $(7,8)^-$, $(6,10)^-$, $(5,16)^-$, and $(9,15)^-$, respectively. The number of basin-hopping steps per temperature varied from 500 000 for the smallest cluster to 50 000 for $N=4352$; results are summarized in Table II. Aside from the $(7,8)^-$ and $(6,10)^-$ constructions basin-hopping located significantly lower minima than previously reported,[51] with improvements up to several atomic units in magnitude. For $N=1632$ and 1902 the I structure remained the lowest one found even after more than 200 000 basin-hopping steps (Fig. 2). It is still possible that lower minima exist; for $N=1382$ a lower minimum was only located after about 150 000 steps. Nevertheless, it seems likely that the rosette motif will play an important role in determining the equilibrium properties of Thomson clusters in this size range and is likely to be found in experimentally realizable systems with spherical topology. All the structures described in this report will be made available for download from the Cambridge Cluster Database.[53]

IV. DISCUSSION

Using the systematic global optimization results in Ref. 39 and the present results for selected sizes we can identify the trends for favored defect structures in more detail (Fig. 3). Most of the putative global minima for $N<300$ simply have 12 disclinations, manifested as 12 isolated five-membered rings (though not necessarily symmetrically arranged) in the Voronoi construction.[39,53] Indeed, for $12\leq N\leq 100$ purely geometric factors can account for most of the few cases of presumed global minima that do not have exactly 12 isolated five-membered rings.[33,54] For $N>300$, and especially as we approach $N=400$, heptagons become increasingly common as a way to relieve strain from the dislocations, in agreement with the predictions of continuum elastic theory.[17,18,52] It was predicted that for $N\sim 530$ isolated five-membered rings without an accompanying pentamer/heptamer defect should become unfavorable.[18] Extended dislocations, consisting of one heptagon and two neighboring pentagons in the face dual, were identified as favorable defects in this regime in our previous report.[39] For $N=582$ and 752, where we have some confidence that we have found the true global minimum, the favored structures contain 12 of these extended dislocations (Fig. 2), giving 24 pentagons and 12 heptagons in the Voronoi representation. The lowest minimum found for $N=942$ contains 12 copies of a twinned grain boundary, where two heptagons share an edge in the Voronoi representation, which was also identified in previous work.[39]

To identify the transition region beyond which isolated disclinations are unfavorable we conducted further global optimization runs for $N=400,410,\ldots,560,570$. In each case

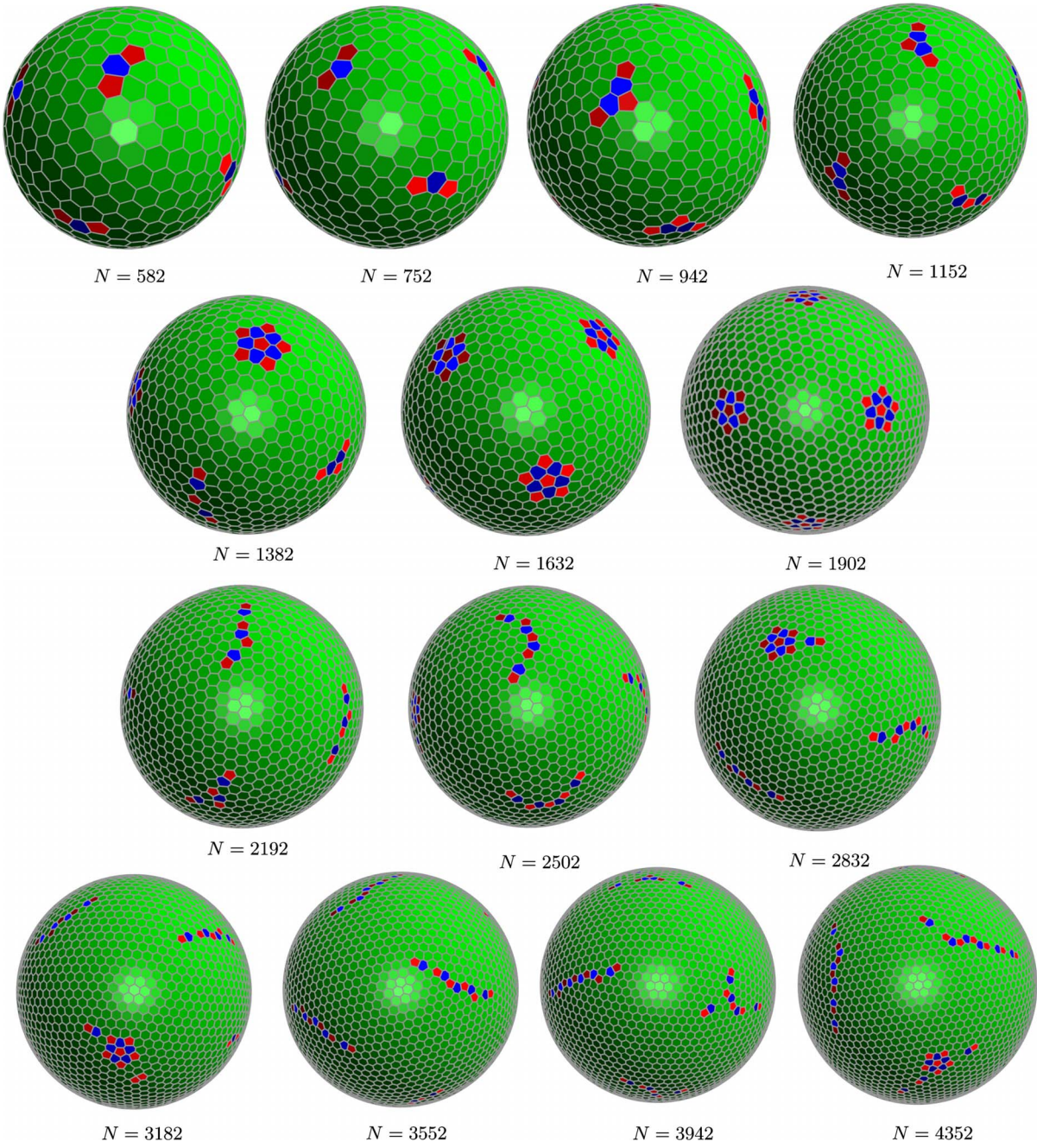

FIG. 2. (Color online) Voronoi representations of the lowest minima located for selected sizes at which local minima with I or I_h symmetry exist for structures with 12 rosettes. The pentagons, hexagons, and heptagons are colored red (medium gray), green (light gray), and blue (dark gray), respectively.

three runs were started from different random starting configurations and continued until all three runs had located the same lowest minimum. This procedure required up to 200 000 basin-hopping steps in some cases. Previous experience with many different systems, including cross validation of basin-hopping results by other methods, suggests that the resulting structures are good candidates for the true global minima. However, we note that exceptions could arise for multifunnel potential energy surfaces, as documented in previous work.[42,43,55] The results are recorded in Table I and selected structures are illustrated in Fig. 1. Nine of these structures improve upon previous results[51] by between 10^{-4} and 18 a.u. No isolated disclinations are found in this data set for $N>520$. It is also noteworthy that most global minima have nontrivial point groups, in agreement with the suggestion that higher-symmetry structures are generally associated with particularly high or particularly low energies.[44,56,57] We expect this trend to extend to larger systems with defects separating into 12 distinct groups related by exact or approximate[44,56,57] symmetry operations. This pattern may also help to minimize strain, in an analogous fashion to the pentagon "repulsion" rule for fullerenes.[58]

Most of the defects for $N=1152$ are again twinned grain boundaries, but we also see a defect with an alternating ar-

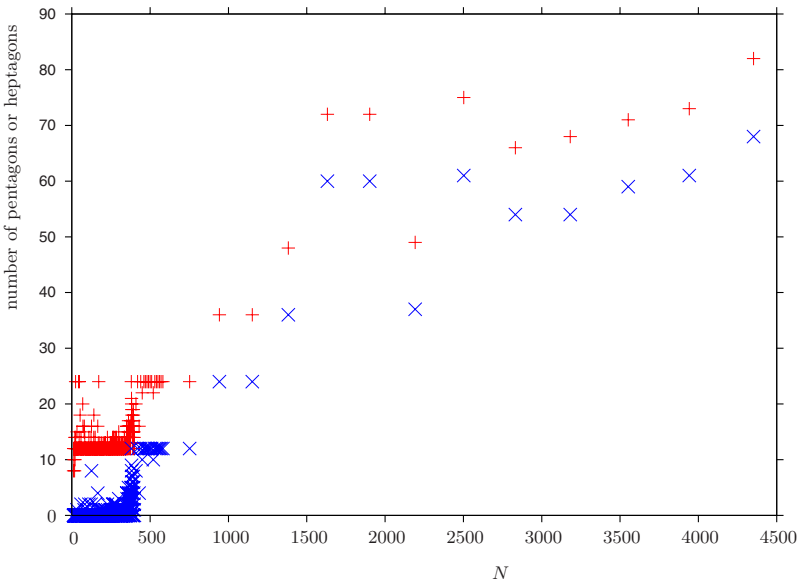

FIG. 3. (Color online) Plot of the number of pentagons (+) and heptagons (×) in the Voronoi representations of the lowest known minima for the Thomson problem. Results for $N \leq 400$ are taken from the structures reported in Ref. 39. The results for $N > 400$ correspond to global optimization results for the sizes in Table II where stable minima exist with I or I_h symmetry for the $(0,k)^-$ series based on 12 rosette defects, along with the results from $N=400$ to $N=570$ in Table I.

rangement of three pentagons and two heptagons. The first putative global minimum in this set to exhibit rosettes occurs at $N=1382$, where the lowest structure located has an additional twinned grain boundary. The energy difference between icosahedral structures and the lowest minimum is smallest for $1000 \leq N \leq 2000$ (Table II). Above this size the lowest structures located have irregular grain boundaries, and some also possess a few rosette defects (Fig. 2). These larger structures are unlikely to be the true global minima but we have performed sufficient sampling to be confident that they are representative of the lowest-lying structures.

Models based on continuum elastic theory have previously been applied to predict trends in defect structure by focusing on screened defect-defect interactions.[24,52] Here the ratio of the disclination core energy to the Young's modulus plays a key role.[52] In the limit of large core defect energy the theory suggests that 12 disclinations will be favored. However, for smaller defect core energies structures with 12 finite grain boundaries are expected to lie lower in energy.[52] For some parameter ranges in this model the grain boundaries exhibit a tendency to spiral, while branching was observed for small core defect energies where the number of defects proliferates.[52] In the present calculations curvature is apparent in some of the grain boundaries for $N=2502$ (Fig. 2), while branching occurs for $N=3942$. However, we have not found any structures that could be described as rosettes (or pentagonal buttons[52]) associated with additional radial dislocations. It has also been suggested[59] that low-energy arrangements might favor dislocations arranged on increasingly straight lines at larger sizes. This regime might occur at sizes beyond those considered in the present work. We have also fitted the quantity $(2E-N^2)/N^{3/2}$ for the putative global minima located in the present work to functions involving inverse powers of N. The fits (data not shown) indicate that our results do not correspond to large enough N for the very large system limit of continuum elastic theory to be reached.[26] Further changes in the favored defect structures corresponding to different levels of organization[60] might be observed before this limit is reached.

Experimental results for self-assembled beads in "colloidosomes" have indicated the formation of grain-boundary scars for systems containing more than around 360 particles,[11] where our results[39] suggest that pentagon-heptagon-pentagon extended dislocations are the most favorable form of defect for the Thomson problem. Hence it seems likely that the rosette motif will appear at still larger sizes in experimental systems that exhibit spherical topology.

The relative stability of icosahedral structures containing 12 rosettes in the size range between $1000 \leq N \leq 2000$ naturally prompts us to consider the stability of the face dual carbon clusters, which contain $20\Delta-120$ atoms. Pérez-Garrido has previously reported results for such structures

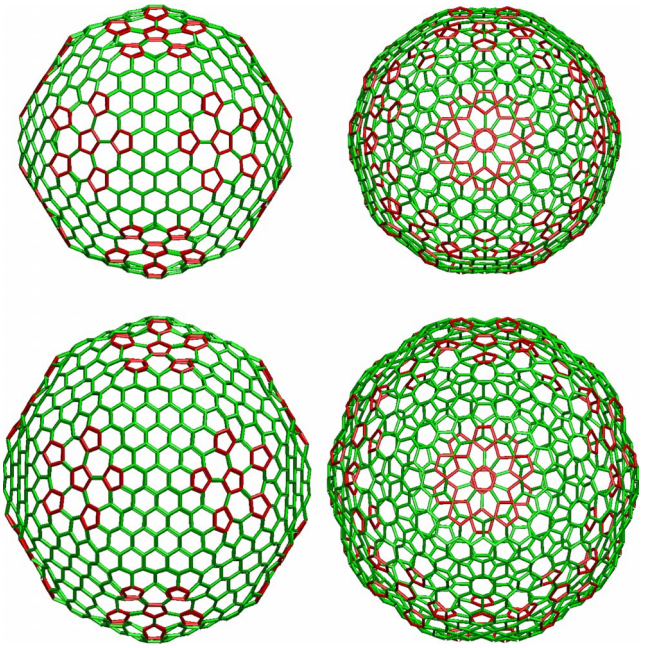

FIG. 4. (Color online) Geometry-optimized C_{860} (top) and C_{1160} (bottom) clusters. Views are shown down the approximate C_2 (left) and C_5 (right) axes with pentagonal rings highlighted in red (light gray).

within the Hückel approximation and using an empirical potential with the carbon atoms constrained to the surface of a sphere.[6] In the present work we have performed energy minimization without constraints for the clusters C_{860} and C_{1160}, starting from idealized face dual structures with I_h symmetry corresponding to $(0,7)^-$ and $(0,8)^-$. The electronic structure was treated using density functional theory, as implemented in the ONETEP package,[61] with the PBE functional,[62] norm-conserving pseudopotentials,[63] and a plane-wave basis cutoff at 500 eV. Periodic boundary conditions were employed for a cubic box of side length 100 a.u. We were able to converge the geometries to a root-mean-square gradient of about 3×10^{-3} a.u. for C_{860} and 7×10^{-4} a.u. for C_{1160}. The clusters relax significantly from the starting geometries where all the atoms lie on a sphere. In particular, there is significant corrugation around each rosette site and slight deviations from perfect I_h symmetry can be detected (Fig. 4). Nevertheless, the corresponding structures represent local minima in each case.

The present results therefore illustrate how systematic global optimization can complement coarse-grained analytic models to identify structural trends at an atomic level of detail. It seems likely that the Thomson problem will continue to provide new insight into the behavior of a wide range of systems with spherical topology.

ACKNOWLEDGMENTS

We acknowledge and greatly appreciated discussions on Thomson's problem with the late Andrew M. Gleason.

[1] N. W. Ashcroft and N. D. Mermin, *Solid State Physics* (Holt-Saunders, Tokyo, 1981).
[2] R. Phillips, *Crystals, Defects and Microstructures* (Cambridge University Press, Cambridge, England, 2001).
[3] D. L. D. Caspar and A. Klug, Cold Spring Harbor Symp. Quant. Biol. **27**, 1 (1962).
[4] C. J. Marzec and L. A. Day, Biophys. J. **65**, 2559 (1993).
[5] H. W. Kroto, J. R. Heath, S. C. O'Brien, R. F. Curl, and R. E. Smalley, Nature (London) **318**, 162 (1985).
[6] A. Pérez-Garrido, Phys. Rev. B **62**, 6979 (2000).
[7] U. Albrecht and P. Leiderer, J. Low Temp. Phys. **86**, 131 (1992).
[8] P. Leiderer, Z. Phys. B: Condens. Matter **98**, 303 (1995).
[9] D. Pum, P. Messner, and U. B. Sleytr, J. Bacteriol. **173**, 6865 (1991).
[10] U. B. Sleytr, M. Sára, D. Pum, and B. Schuster, Prog. Surf. Sci. **68**, 231 (2001).
[11] A. R. Bausch, A. C. M. J. Bowick, A. D. Dinsmore, M. F. Hsu, D. R. Nelson, M. G. Nikolaides, A. Travesset, and D. A. Weitz, Science **299**, 1716 (2003).
[12] P. Lipowsky, M. J. Bowick, J. H. Meinke, D. R. Nelson, and A. R. Bausch, Nature Mater. **4**, 407 (2005).
[13] T. Einert, P. Lipowsky, J. Schilling, M. J. Bowick, and A. R. Bausch, Langmuir **21**, 12076 (2005).
[14] N. J. A. Sloane, Sci. Am. **250**, 116 (1984).
[15] J. H. Conway and N. J. A. Sloane, *Sphere Packings*, 3rd ed. (Springer-Verlag, New York, 1998).
[16] Y.-S. Cho, G.-R. Yi, J.-M. Lim, S.-H. Kim, V. N. Manoharan, D. J. Pine, and S.-M. Yang, J. Am. Chem. Soc. **127**, 15968 (2005).
[17] M. J. W. Dodgson, J. Phys. A **29**, 2499 (1996).
[18] M. J. W. Dodgson and M. A. Moore, Phys. Rev. B **55**, 3816 (1997).
[19] Y. Masuda, T. Itoh, and K. Koumoto, Adv. Mater. **17**, 841 (2005).
[20] K. Simons and W. L. C. Vaz, Annu. Rev. Biophys. Biomol. Struct. **33**, 269 (2004).
[21] D. R. Nelson, *Defects and Geometry in Condensed Matter Physics* (Cambridge University Press, Cambridge, England, 2002).
[22] A. Pérez-Garrido and M. A. Moore, Phys. Rev. B **60**, 15628 (1999).
[23] A. M. Livshits and Y. E. Lozovik, Chem. Phys. Lett. **314**, 577 (1999).
[24] M. Bowick, A. Cacciuto, D. R. Nelson, and A. Travesset, Phys. Rev. Lett. **89**, 185502 (2002).
[25] E. L. Altschuler and A. Perez-Garrido, Phys. Rev. E **73**, 036108 (2006).
[26] M. J. Bowick, A. Cacciuto, D. R. Nelson, and A. Travesset, Phys. Rev. B **73**, 024115 (2006).
[27] T. Dumitrica, M. Hua, and B. I. Yakobson, Proc. Natl. Acad. Sci. U.S.A. **103**, 6105 (2006).
[28] W. F. Harris and L. E. Scriven, Nature (London) **228**, 827 (1970).
[29] W. F. Harris, Philos. Mag. **32**, 37 (1975).
[30] J. Thomson, Philos. Mag. **7**, 237 (1904).
[31] L. T. Wille, Nature (London) **324**, 46 (1986).
[32] T. Erber and G. M. Hockney, J. Phys. A **24**, L1369 (1991).
[33] E. L. Altschuler, T. J. Williams, E. R. Ratner, F. Dowla, and F. Wooten, Phys. Rev. Lett. **72**, 2671 (1994).
[34] T. Erber and G. M. Hockney, Phys. Rev. Lett. **74**, 1482 (1995).
[35] E. L. Altschuler, T. J. Williams, E. R. Ratner, R. Tipton, R. Stong, F. Dowla, and F. Wooten, Phys. Rev. Lett. **78**, 2681 (1997).
[36] J. R. Morris, D. M. Deaven, and K. M. Ho, Phys. Rev. B **53**, R1740 (1996).
[37] E. L. Altschuler and A. Pérez-Garrido, Phys. Rev. E **71**, 047703 (2005).
[38] T. Erber and G. M. Hockney, Adv. Chem. Phys. **98**, 495 (1997).
[39] D. J. Wales and S. Ulker, Phys. Rev. B **74**, 212101 (2006).
[40] Z. Li and H. A. Scheraga, Proc. Natl. Acad. Sci. U.S.A. **84**, 6611 (1987).
[41] Z. Li and H. A. Scheraga, J. Mol. Struct. **179**, 333 (1988).
[42] D. J. Wales and J. P. K. Doye, J. Phys. Chem. A **101**, 5111 (1997).
[43] D. J. Wales and H. A. Scheraga, Science **285**, 1368 (1999).
[44] D. J. Wales, *Energy Landscapes* (Cambridge University Press, Cambridge, England, 2003).
[45] F. H. Stillinger and T. A. Weber, Science **225**, 983 (1984).
[46] D. J. Wales and J. P. K. Doye, J. Chem. Phys. **119**, 12409 (2003).
[47] J. P. K. Doye, D. J. Wales, and R. S. Berry, J. Chem. Phys. **103**, 4234 (1995).

[48] J. P. K. Doye and D. J. Wales, Science **271**, 484 (1996).
[49] J. P. K. Doye and D. J. Wales, J. Chem. Soc., Faraday Trans. **93**, 4233 (1997).
[50] Http://www-wales.ch.cam.ac.uk/software.html
[51] M. Bowick, C. Cecka, and A. Middleton, http://physics.syr.edu/condensedmatter/thomson/thomson.htm
[52] M. J. Bowick, D. R. Nelson, and A. Travesset, Phys. Rev. B **62**, 8738 (2000).
[53] D. J. Wales, J. P. K. Doye, A. Dullweber, M. P. Hodges, F. Y. Naumkin, F. Calvo, J. Hernández-Rojas, and T. F. Middleton, http://www-wales.ch.cam.ac.uk/CCD.html
[54] J. R. Edmundson, Acta Crystallogr. **48**, 60 (1992).
[55] J. P. K. Doye, M. A. Miller, and D. J. Wales, J. Chem. Phys. **110**, 6896 (1999).
[56] D. J. Wales, Chem. Phys. Lett. **285**, 330 (1998).
[57] D. J. Wales, Chem. Phys. Lett. **294**, 262 (1998).
[58] H. W. Kroto, Nature (London) **329**, 529 (1987).
[59] A. Pérez-Garrido, M. J. W. Dodgson, and M. A. Moore, Phys. Rev. B **56**, 3640 (1997).
[60] P. W. Anderson, Science **177**, 393 (1972).
[61] C.-K. Skylaris, P. D. Haynes, A. A. Mostofi, and M. C. Payne, J. Chem. Phys. **122**, 084119 (2005).
[62] J. P. Perdew, K. Burke, and M. Ernzerhof, Phys. Rev. Lett. **77**, 3865 (1996).
[63] M. C. Payne, M. P. Teter, D. C. Allan, T. A. Arias, and J. D. Joannopoulos, Rev. Mod. Phys. **64**, 1045 (1992).